SLAC-PUB-7204
DESY 96-126
July 1996

Gluon Radiation in Diffractive Electroproduction*

W. Buchmüller, M. F. McDermott
Deutsches Elektronen-Synchrotron DESY, 22603 Hamburg, Germany
and
A. Hebecker
Stanford Linear Accelerator Center, Stanford University, Stanford, CA 94309

Abstract

Order α_s-corrections to the diffractive structure functions F_L^D and F_2^D at large Q^2 and small x are evaluated in the semiclassical approach, where the initial proton is treated as a classical colour field. The diffractive final state contains a fast gluon in addition to a quark-antiquark pair. Two of these partons may have large transverse momentum. Our calculations lead to an intuitive picture of deep-inelastic diffractive processes which is very similar to Bjorken's aligned-jet model. Both diffractive structure functions contain leading twist contributions from high-$p_\perp$ jets.

(Submitted for Publication)

*Work partially supported by the Department of Energy, contract DE-AC03-76SF00515.

1 Introduction

The large-rapidity-gap events, observed in deep inelastic scattering at HERA [1, 2], are a puzzling phenomenon. As the data show, the cross section for these 'diffractive' events is not suppressed at large values of Q^2 relative to the inclusive cross section, i.e., these events represent a 'leading twist' contribution to the inclusive structure function. However, since the initial proton escapes essentially unscathed, they cannot be described by ordinary perturbation theory within the parton model. One may therefore hope that the study of deep inelastic diffractive processes will lead to a deeper understanding of the interplay between 'soft' and 'hard' processes in QCD.

A theory of hard diffractive processes, which does not yet exist, has to provide a clean separation between the perturbative and the non-perturbative aspects of the scattering process. In particular, it should explain why the large-rapidity-gap events are a 'leading twist' phenomenon, and it should yield a quantitative description of at least some aspects of the diffractive structure functions. At present the basic mechanism responsible for hard diffraction has not yet been unequivocally identified. Several phenomenological approaches have been developed which may be partially interrelated. These include the aligned-jet model [3] (whose origin dates back before the development of QCD), the idea of a 'pomeron' structure function [4], perturbative 2-gluon exchange [5] and partonic models supplemented by soft colour interactions [6, 7].

Recently, a semiclassical approach to diffractive deep inelastic scattering has been proposed [8]. In the proton rest frame the dominant process is the dissociation of the virtual photon into a quark antiquark pair, and further gluons and quark pairs generated by radiation, which then interact with the proton[1]. The basic idea of the semiclassical approach is to treat the proton at small values of x, where the momentum transfer is generally small, as a classical colour field localized within a radius $1/\Lambda_{QCD}$. Deep inelastic scattering is then viewed as scattering of this system of fast quarks and gluons off the classical colour field. If this system happens to be in a colour singlet state after the interaction one obtains a 'diffractive' final state with a large rapidity gap between the fast proton and the diffractive hadronic system. Otherwise, an ordinary non-diffractive final state is produced.

In [8] the dominant contributions to inclusive and diffractive structure functions, due

[1] For a discussion and references, see [9].

to a virtual quark-antiquark initial state, were calculated. The results depend on non-perturbative averages over the colour field inside the proton. Here we compute $\mathcal{O}(\alpha_s)$-corrections to these results by taking the radiation of a gluon in the initial state into account. This allows us to discuss the cross section for the production of high-$p_\perp$ jets. Furthermore, we will clarify the connection of our approach to previous work on pair production in external fields based on light-cone quantization [10].

The paper is organized as follows. In Sect. 2 we discuss the applicability of the semiclassical approach to high energy diffractive scattering. In Sect. 3 we then rederive the results obtained in [8] in a way closely related to the techniques used in [10]. This calculation is extended to the case of an initial quark-antiquark-gluon system in Sect. 4 with emphasis on the production of high-$p_\perp$ jets. Our results are summarized in Sect. 5, and some details of the calculations we performed are explained in the appendices.

2 Semiclassical approach to high-energy scattering

The subject of the present paper is the analysis of diffractive deep inelastic scattering in terms of the production of quark-antiquark and quark-antiquark-gluon final states. These processes are considered in the small-x or high-energy limit, where a considerable part of the total $\gamma^* p$ cross section is diffractive. The gluon densities are known to grow rapidly in this small-x region. Therefore, as already discussed in [8], a description of the proton in terms of a classical colour field should be adequate. This is closely related to the description of high energy processes in terms of Wilson lines, which has been discussed by several authors [11, 12]. In this section the basis of the semiclassical approach shall be discussed in more detail. It is similar to the method developed by Balitsky [13] for small-x deep inelastic scattering. However, in the following more emphasis shall be placed on the connection with the proton wave functional in the Schrödinger picture.

To keep the discussion as simple as possible, consider first the elastic scattering of a quark off a proton. Although this process is unphysical since quarks are confined, it can serve to illustrate the method of calculation. Therefore, in the following confinement is ignored and quarks are treated as asymptotic states. The generalization to the physical case of diffractive electroproduction is straightforward and will be discussed subsequently.

The scattering of a point-like quark with initial momentum q off a relativistic bound state with initial momentum p is illustrated in Fig. 1. Let m_p be the proton mass,

and s and t the usual Mandelstam variables for a $2 \to 2$ process. In the high-energy limit, $s \gg t,\, m_p^2$, the contribution from the annihilation of the incoming quark with a constituent quark of the proton is negligible. The amplitude is dominated by diagrams with a fermion line going directly from the initial to the final quark state. Therefore, the proton can be described by a Schrödinger wave functional $\Phi_p[A]$ (cf. [14]) depending on the gluon field only. Quarks are integrated out, yielding a modification of the gluonic action.

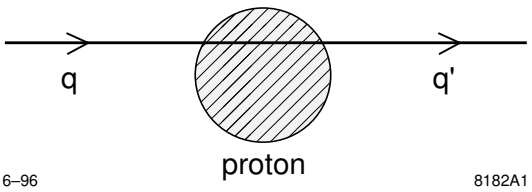

Fig.1 Scattering of a point-like quark off the proton bound state.

For a scattering process the amplitude can be written in the proton rest frame as

$$< q'p'|qp >= \lim_{T\to\infty} \int DA_T DA_{-T} \Phi^*_{p'}[A_T]\Phi_p[A_{-T}] \int_{A_{-T}}^{A_T} DA\, e^{iS[A]} < q'|q >_A \ . \qquad (1)$$

Here the fields A_{-T} and A_T are defined on three-dimensional surfaces at constant times $-T$ and T, and A is defined in the four-dimensional region bounded by these surfaces. The field A has to coincide with A_{-T} and A_T at the boundaries and the action S is defined by an integration over the domain of A. The amplitude $< q'|q >_A$ describes the scattering of a quark by the given external field A.

The initial state proton, having well defined momentum $\vec{p}$, is not well localized in space. However, the dominant field configurations in the proton wave functional are localized on a scale $\Lambda \sim \Lambda_{QCD}$. Also the field configurations $A(\vec{x},t)$, which interpolate between initial and final proton state, are localized in space at each time t. Assume that the incoming quark wave packet is localized such that it passes the origin $\vec{x}=0$ at time $t=0$. At this instant the field configuration $A(\vec{x},t)$ is centered at

$$\vec{x}[A] \equiv \int d^3\vec{x} E_A(\vec{x}) \cdot \vec{x} \Big/ \int d^3\vec{x} E_A(\vec{x})\,, \qquad (2)$$

where $E_A(\vec{x})$ is the energy density of the field $A(\vec{x},t)$ at $t=0$. The amplitude (1) can now be written as

$$< q'p'|qp >= \lim_{T\to\infty} \int d^3\vec{x} \int DA_T DA_{-T} \Phi^*_{p'}\Phi_p \int_{A_{-T}}^{A_T} DA\, e^{iS} \delta^3(\vec{x}[A]-\vec{x}) < q'|q >_A \ . \qquad (3)$$

Using the transformation properties under translations,

$$<q'|q>_{L_{\vec{x}}A} = e^{i(\vec{q}-\vec{q}')\vec{x}} <q'|q>_A \quad , \quad \Phi^*_{p'}[L_{\vec{x}}A]\Phi_p[L_{\vec{x}}A] = e^{i(\vec{p}-\vec{p}')\vec{x}}\Phi^*_{p'}[A]\Phi_p[A] \; , \tag{4}$$

where

$$L_{\vec{x}}A(\vec{y}) \equiv A(\vec{y}-\vec{x}) \, , \tag{5}$$

one obtains,

$$<q'p'|qp> = 2m_p(2\pi)^3\delta^3(\vec{p}\,' + \vec{q}\,' - \vec{p} - \vec{q}) \int_A <q'|q>_A \; . \tag{6}$$

Here $\int_A$ denotes the operation of averaging over all field configurations contributing to the proton state which are localized at $\vec{x} = 0$ at time $t = 0$. It is defined by

$$\int_A F \equiv \frac{1}{2m_p} \lim_{T\to\infty} \int DA_T DA_{-T} \Phi^*_{p'}\Phi_p \int_{A_{-T}}^{A_T} DA \, e^{iS}\delta^3(\vec{x}[A])F[A] \tag{7}$$

for any functional F. The normalization $\int_A \; 1 = 1$ follows from

$$<p'|p> = 2p_0(2\pi)^3\delta^3(\vec{p}\,' - \vec{p}\,) \; . \tag{8}$$

More complicated processes can be treated in complete analogy as long as the proton scatters elastically. In particular, the above arguments apply to the creation of colour singlet quark antiquark pairs [8]

$$<q\bar{q}p'|\gamma^* p> = 2m_p(2\pi)^3\delta^3(\vec{k}_f - \vec{k}_i) \int_A <q\bar{q}|\gamma^*>_A \, , \tag{9}$$

where $\vec{k}_i$ and $\vec{k}_f$ are the sums of the momenta in the initial and final states respectively. The generalization of this simplest diffractive process to a process with an additional fast final state gluon, $\gamma^* \to q\bar{q}g$, will be given in Sect. 4. In contrast to the quark-proton scattering discussed above, here a colour neutral state is scattered off the proton. Therefore no immediate contradiction with colour confinement arises. However, it has to be assumed that the hadronization of the produced partonic state takes place after the interaction with the proton, which is described in terms of fast moving partons.

When calculating the cross section from Eq. (9) the square of the momentum conserving δ-function translates into one momentum conserving δ-function using Fermi's trick. This δ-function disappears after the momentum integration for the final state proton, resulting in a cross section formula identical to scattering by an external field.

From the above discussion a simple recipe for the calculation of diffractive processes at high energy follows:

The partonic process is calculated in a given external colour field, localized at $\vec{x} = 0$ at time $t = 0$. The weighted average over all colour fields contributing to the proton state is taken on the amplitude level. We assume that the typical contributing field is smooth on a scale Λ and is localized in space on the same scale Λ. Finally, the cross section is calculated using standard formulae for the scattering off an external field.

For the comparison of diffractive and inclusive structure functions it is important to know whether the above semiclassical picture also applies to non-singlet partonic final states, e.g. to the production of a colour-octet $q\bar{q}$-pair. In this situation the definition of some analog of the 'averaging'-operator in terms of a path integral and the proton wave functional is not obvious. The problem is that the fragmentation will in general involve both the diffractively produced final state and the proton remnant. Below we shall assume that such processes can still be described by calculating the partonic amplitude in a smooth localized colour field and by taking an appropriate average over different field configurations at the end.

3 Quark pair production in a colour field

The basic process in deep inelastic scattering, viewed in the proton rest frame, is the dissociation of a virtual photon into a quark antiquark pair which then interacts with the proton. The corresponding scattering amplitude reads (cf. [8])

$$S_\mu = ie \int d^4x e^{-iqx} \bar{\psi}_u(x) \gamma_\mu \psi_v(x) \ , \tag{10}$$

where ψ_u and ψ_v are the wave functions of the outgoing quark and antiquark depending on the momenta p' and l', respectively, and e is the electric charge (cf. Fig. 2).

In the semiclassical approximation the interaction with the proton is treated as scattering in a classical colour field $G_\mu(x) = T^a G^a_\mu(x)$, $T^a = \frac{1}{2}\lambda^a$. The quark and antiquark wave functions are solutions of the Dirac equation with the colour field. Hence, they satisfy the integral equations

$$\psi_v(x) = \psi_v^{(0)}(x) - \int d^4x' S_F(x - x') \not{G}(x') \psi_v(x') \ , \tag{11}$$

$$\bar{\psi}_u(x) = \bar{\psi}_u^{(0)}(x) - \int d^4x' \bar{\psi}_u(x') \not{G}(x') S_F(x' - x) \ . \tag{12}$$

Here $\psi_v^{(0)}$ and $\bar{\psi}_u^{(0)}$ are solutions of the free Dirac equation. In the following we will explicitly consider only those contributions to S_μ in which both the quark and antiquark interact with the field G_μ.

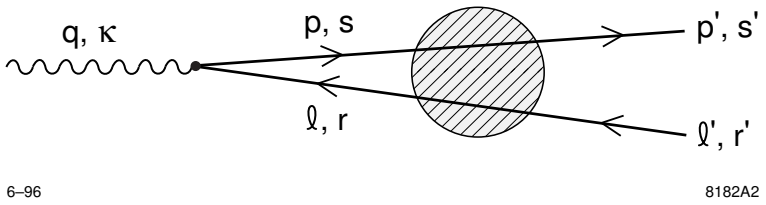

Fig.2 Quark pair production in the colour field of the proton.

Inserting these equations into the amplitude (10), using the Fourier decomposition of the free propagator S_F and performing the integration over the position of the photon vertex, one obtains

$$S_\mu = -ie \int \frac{d^4p}{(2\pi)^4} \int d^4x \bar{\psi}_u(x) \not{G}(x) e^{-ipx} \frac{1}{\not{p} - m} \gamma_\mu \frac{1}{\not{l} + m} \int d^4y e^{-ily} \not{G}(y) \psi_v(y) \ , \qquad (13)$$

where $l = q - p$. Explicit expressions for $\bar{\psi}_u$ and ψ_v have been obtained in a high-energy expansion for an arbitrary soft colour field [8].

We are interested in deep inelastic scattering at small x, where quark and antiquark have large momenta in the proton rest frame. Hence, the propagators in Eq. (13) can be treated in a high-energy approximation. It is convenient to introduce light-cone variables, e.g.,

$$l_+ = l^0 + l^3 \ , \ l_- = l^0 - l^3 \ , \ \bar{l}_- = \frac{l_\perp^2 + m^2}{l_+} \ . \qquad (14)$$

Here $\bar{l}_\mu$ denotes the momentum vector whose "–"-component satisfies the mass shell condition. The propagators in Eq. (13) can be written as

$$\frac{1}{\not{l} + m} = \frac{\sum_r v_r(\bar{l}) \bar{v}_r(\bar{l})}{l_+(l_- - \bar{l}_-) + i\epsilon} + \frac{\gamma_+}{2l_+} \ , \qquad (15)$$

$$\frac{1}{\not{p} - m} = \frac{\sum_s u_s(\bar{p}) \bar{u}_s(\bar{p})}{p_+(p_- - \bar{p}_-) + i\epsilon} + \frac{\gamma_+}{2p_+} \ . \qquad (16)$$

To obtain the first term in a high energy expansion of the scattering amplitude S_μ one can drop the terms proportional to γ_+ in Eqs. (15),(16).

In the high energy expansion the leading term for the wave functions ψ_v and $\bar{\psi}_u$ is the product of a non-abelian eikonal factor and a plane wave solution of the Dirac equation

[11]. The scattering amplitude (13) then takes the form of a product of the photon-quark-antiquark vertex, propagator factors and two matrix elements of an effective gluon vertex between on-shell spinors. These matrix elements describe the elastic scattering between the high energy (anti)quark and the proton, as discussed in Sect. 2. They are evaluated in Appendix A. For a soft gluon field inside the proton one finds for the matrix element of the antiquark

$$\begin{aligned} T_{r,r'}(l,l') &= \int d^4y\ \bar{v}_r(l) e^{-ily} \not{G}(y) \psi_v(y) \\ &\simeq -2\pi i\ 2l_+ \delta_{rr'} \delta(l_+ - l'_+) \left(\tilde{F}(l_\perp - l'_\perp) - (2\pi)^2 \delta^2(l_\perp - l'_\perp) \right) , \end{aligned} \tag{17}$$

where

$$\begin{aligned} \tilde{F}(l_\perp - l'_\perp) &= \int_{y_\perp} e^{i(l_\perp - l'_\perp) y_\perp} F(y_\perp) , \\ F(y_\perp) &= P \exp\left(\frac{i}{2} \int_{-\infty}^{\infty} dy_+ G_-(y_+, y_-, y_\perp) \right) . \end{aligned} \tag{18}$$

$F(y_\perp)$ is the eikonal factor of the antiquark trajectory. If the colour field of the proton is 'soft' the dependence on y_- can be neglected. For the corresponding matrix element of the quark one finds

$$\begin{aligned} \int d^4y\ \bar{\psi}_u(y) \not{G}(y) u_s(\bar{p}) e^{-ipy} &\simeq 2\pi i\ 2p_+ \delta_{s's} \delta(p'_+ - p_+) \left(\tilde{F}^\dagger(p'_\perp - p_\perp) - (2\pi)^2 \delta^2(p'_\perp - p_\perp) \right) \\ &= T^\dagger_{s's}(p', p) . \end{aligned} \tag{19}$$

Inserting these matrix elements into Eq. (13) and adding the contributions where one of the particles is not scattered one obtains, after performing the p_--integration,

$$\begin{aligned} \bar{S}_\mu &= \frac{e}{\pi}\ q_+ \delta(q_+ - p'_+ - l'_+) \int d^2 l_\perp\ \frac{\alpha(1-\alpha)}{N^2 + l_\perp^2}\ \bar{u}_{s'}(p) \gamma_\mu v_{r'}(l) \\ &\qquad \left(\tilde{F}^\dagger(p'_\perp - p_\perp) \tilde{F}(l_\perp - l'_\perp) - (2\pi)^4 \delta^2(p'_\perp - p_\perp) \delta^2(l_\perp - l'_\perp) \right) \\ &\equiv -4\pi\ \delta(q_+ - p'_+ - l'_+)\ T_\mu , \end{aligned} \tag{20}$$

where

$$p'_+ = (1-\alpha)\ q_+ ,\ l'_+ = \alpha\ q_+ ,\ N^2 = \alpha(1-\alpha) Q^2 + m^2 . \tag{21}$$

In the following it will turn out to be useful to restrict the integrand in Eq. (20) to configurations with $\alpha < 1/2$, where the quark is faster than the antiquark.

The non-perturbative interaction with the proton is contained in $\tilde{F}$, the Fourier transform of the eikonal factor. The product of eikonal factors appearing in Eq. (20)

may be expressed as Fourier transform with respect to the transverse distance between quark and antiquark. Introducing

$$W_{x_\perp}(y_\perp) = F^\dagger(x_\perp)F(x_\perp + y_\perp) - 1 \ , \tag{22}$$

one has

$$\begin{aligned}
\tilde{F}^\dagger(p'_\perp - p_\perp)\tilde{F}(l_\perp - l'_\perp) &= \int_{x_\perp, z_\perp} e^{i(p_\perp - p'_\perp)x_\perp} e^{i(l_\perp - l'_\perp)z_\perp} F^\dagger(x_\perp)F(z_\perp) \\
&= \int_{x_\perp, y_\perp} e^{-i\Delta_\perp x_\perp} e^{i(l_\perp - l'_\perp)y_\perp} \ (W_{x_\perp}(y_\perp) + 1) \\
&= \int_{x_\perp} e^{-i\Delta_\perp x_\perp} \ \left(\tilde{W}_{x_\perp}(l_\perp - l'_\perp) + (2\pi)^2\delta^2(l_\perp - l'_\perp)\right) \ . \qquad (23)
\end{aligned}$$

Here $\Delta_\perp = p'_\perp + l'_\perp$ is the transverse momentum transfer from the proton. We assume that the colour field of the proton is smooth on a scale Λ, which implies that $\tilde{W}_{x_\perp}(k_\perp)$ falls off exponentially with increasing $k_\perp^2/\Lambda^2$.

Cross sections and structure functions can now be evaluated in the standard manner (cf. [8]). The deep inelastic cross sections are given by

$$d\sigma_{\mu\nu} = \frac{2\pi}{q_+} \ T^*_\mu T_\nu \ d\Phi^{(2)} \ , \tag{24}$$

where $d\Phi^{(2)}$ is the phase space factor. Different projections with respect to Lorentz and colour structure yield longitudinal and transverse, diffractive and inclusive structure functions.

Consider first the inclusive longitudinal structure function F_L. We use the conventional kinematic variables $\xi = x/\beta = x(Q^2 + M^2)/Q^2$, where M^2 is the invariant mass of the produced quark-antiquark pair and $m = 0$. A straightforward calculation, described in Appendix B, yields

$$\begin{aligned}
dF_L &= \frac{Q^2}{\pi e^2} \ d\sigma_L \\
&= \frac{4 \ Q^6}{(2\pi)^7 \beta} \ \frac{d\xi}{\xi} \ d\alpha(\alpha(1-\alpha))^3 \ \int_{x_\perp} \left| \int d^2 l_\perp \frac{\tilde{W}_{x_\perp}(l_\perp - l'_\perp)}{N^2 + l_\perp^2} \right|^2 \ . \qquad (25)
\end{aligned}$$

Note that only a single integration over transverse coordinates occurs. This is a consequence of the δ-function induced by the phase space integration over $\Delta_\perp$ in Eq. (24). Since the form factor $\tilde{W}_{y_\perp}(l_\perp - l'_\perp)$ falls off exponentially with increasing momentum

transfer, one can expand the integrand around $l_\perp = l'_\perp$. This leads to the final result

$$\begin{aligned} F_L &= \frac{2}{\pi^3} \int_x^1 \frac{d\xi}{\xi} \int_0^{1/2} d\alpha \; \beta^2(1-\beta) \int_{x_\perp} | \, \partial_\perp W_{x_\perp}(0) \, |^2 \\ &= \frac{1}{6\pi^3} \int_{x_\perp} | \, \partial_\perp W_{x_\perp}(0) \, |^2 \quad . \end{aligned} \tag{26}$$

The inclusive transverse structure function F_T can be evaluated in a similar way. In the perturbative region $\alpha > \Lambda^2/Q^2$, where the antiquark is sufficiently fast, one obtains

$$\begin{aligned} dF_T &= \frac{Q^2}{\pi e^2} \, d\sigma_T = dF_2 - dF_L \\ &= \frac{1}{8\pi^3} \, \frac{d\xi}{\xi} \, d\alpha \, \frac{\alpha^2 + (1-\alpha)^2}{\alpha(1-\alpha)} \, \beta(\beta^2 + (1-\beta)^2) \int_{x_\perp} | \, \partial_\perp W_{x_\perp}(0) \, |^2 \quad . \end{aligned} \tag{27}$$

The integration over α above the infrared cutoff $\alpha_{min} = \Lambda^2/Q^2$ yields

$$\int_{\alpha_{min}}^{1/2} d\alpha \, \frac{\alpha^2 + (1-\alpha)^2}{\alpha(1-\alpha)} \simeq \ln \frac{Q^2}{\Lambda^2} - 1 \; . \tag{28}$$

From the general expression for F_T (cf. Appendix B) one can easily see that there is also a non-perturbative contribution from the range $\alpha \leq \Lambda^2/Q^2$ which, to leading order in $1/Q^2$, is given by a function of β only. We thus obtain the final result

$$\begin{aligned} F_T &= \frac{1}{4\pi^3} \int_x^1 \frac{d\xi}{\xi} \left(\beta(\beta^2 + (1-\beta)^2) \left(\ln \frac{Q^2}{\Lambda^2} - 1 \right) \int_{x_\perp} | \, \partial_\perp W_{x_\perp}(0) \, |^2 \; + f(\beta) \right) \\ &= \frac{1}{6\pi^3} \ln \frac{Q^2}{\Lambda^2} \int_{x_\perp} | \, \partial_\perp W_{x_\perp}(0) \, |^2 \; + C \; , \end{aligned} \tag{29}$$

where C is an unknown constant. Results for the production of electron-positron pairs in an electromagnetic field, which are completely analogous to Eqs. (26) and (29), have previously been obtained by Bjorken, Kogut and Soper [10] using light-cone quantization.

Let us finally evaluate the diffractive structure functions. In our approach they are determined by the projection onto a colour singlet final state which corresponds to the substitution

$$W_{x_\perp}(y_\perp) \to \frac{1}{\sqrt{3}} \, \mathrm{tr}[W_{x_\perp}(y_\perp)] \; . \tag{30}$$

There is no non-perturbative contribution to F_L to leading order in $1/Q^2$. Further, from the definition of the colour matrix $W_{x_\perp}(y_\perp)$ it is clear that

$$\partial_\perp \mathrm{tr}[W_{y_\perp}(0)] = 0 \; . \tag{31}$$

This immediately implies

$$F_L^D(x, Q^2, \xi) = 0 \ . \tag{32}$$

Like the transverse inclusive structure function, the transverse diffractive structure function also has a non-perturbative contribution. The result can be written in the form (cf. Appendix B)

$$F_2^D(x, Q^2, \xi) = \frac{\beta}{\xi} \bar{F}(\beta) \ , \tag{33}$$

with

$$\bar{F}(\beta) = \frac{4}{3(2\pi)^7} \int d\rho \rho^3 \int_{x_\perp} \left| \int d^2 k_\perp \ \frac{k_\perp + e_\perp \rho \sqrt{1-\beta}}{\beta \rho^2 + (k_\perp + e_\perp \rho \sqrt{1-\beta})^2} \mathrm{tr}[\tilde{W}_{x_\perp}(k_\perp)] \right|^2 \ . \tag{34}$$

Here $e_\perp$ is an arbitrary unit vector whose direction is irrelevant due to rotational invariance. The function $\bar{F}(\beta)$ approaches a finite limit as $\beta \to 0$, as well as $\beta \to 1$.

The results of this section essentially coincide with [8]. There is, however, a difference concerning the β-spectrum of the diffractive contribution. In the space-time picture of [8] the change of direction of the outgoing quarks by their interaction with the proton was not treated sufficiently accurately. This oversimplification led to the conclusion that the β-spectrum depends on the proton structure only via two unknown constants. The present calculation shows that the β-spectrum is entirely non-perturbative and can only be given in terms of an integral which depends on the proton field.

The results for F_2 and F_L correspond to the perturbative contribution of photon-gluon fusion with a gluon density $xg(x) = \text{const.}$, i.e. a classical bremsstrahl spectrum. The diffractive structure function F_2^D is due to purely non-perturbative contributions, where either the quark or the antiquark are soft. This is analogous to modern views of the aligned-jet model [15, 16, 17, 18]. We also note that the slope of F_2 in x is larger by one unit than the slope of F_2^D in ξ. This property of the structure functions has previously been discussed in [6, 8, 19].

4 Radiation of an additional gluon

4.1 Amplitude

In this section the process $\gamma^* \to q\bar{q}g$ in an external colour field is calculated in the kinematical region with two final state partons having high transverse momentum. This

extends the analysis of the previous section (see also [8]) to the case where an additional fast gluon is radiated. The interaction of the gluon with the external field is treated in the high-energy approximation in analogy to the two quarks.

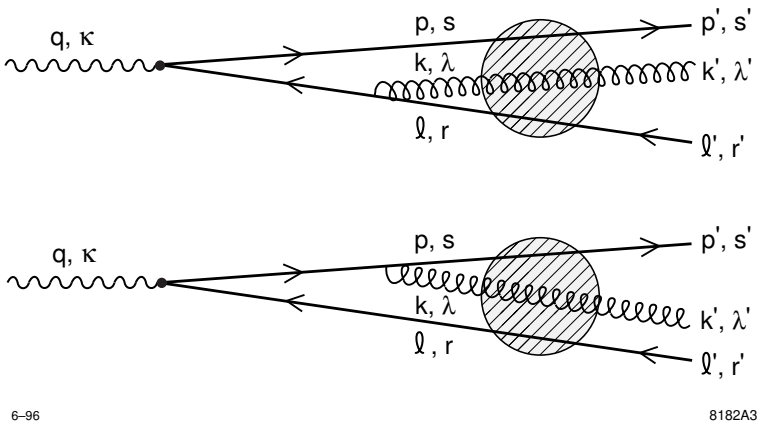

Fig.3 Diagrams for the process $\gamma^* \to q\bar{q}g$.

The amplitude is given by the sum of the two diagrams shown in Fig. 3. Separating explicitly the part which describes the scattering of the gluon off the external field, the amplitude can be given in the form

$$S_\mu^b = \int \frac{d^4k}{(2\pi)^4} A_{\mu\nu}^a \frac{-ig^{\nu\rho}}{k^2} B_{\rho\sigma}^{ab} \varepsilon_{(\lambda')}^{*\sigma}(k') \,. \tag{35}$$

Here A refers to the production of the $q\bar{q}g$-system, including the interactions of the quarks with the external field, and B describes the scattering of the gluon. Like the amplitude S_μ defined in Sect. 3, S_μ^b is a 3×3 colour matrix. The index b denotes the colour of the outgoing gluon.

Using the approximate k_--independence of B, which is analogous to the quark scattering amplitude of the previous section, the k_--integration in Eq. (35) can be performed in such a way that the gluon propagator goes on shell. Since A and B are now physical amplitudes and therefore gauge invariant, only physical polarizations contribute to the gluon propagator connecting A and B,

$$S_\mu^b = \sum_{\lambda=1,2} \int \frac{dk_+ d^2k_\perp}{2(2\pi)^3} A_{\mu\nu}^a \epsilon_{(\lambda)}^{*\nu}(k) \frac{1}{k_+} \epsilon_{(\lambda)}^{\rho}(k) B_{\rho\sigma}^{ab} \varepsilon_{(\lambda')}^{*\sigma}(k') \,. \tag{36}$$

The expression for the high-energy scattering of the gluon is very similar to the analogous

expression for the quark given in the previous section,

$$\begin{aligned} T^g_{\lambda'\lambda}(k,k') &= \epsilon^{\rho}_{(\lambda)}(k) B_{\rho\sigma} \varepsilon^{*\sigma}_{(\lambda')}(k') \\ &= 2\pi i \, 2k_+ \delta_{\lambda'\lambda} \delta(k'_+ - k_+)(\tilde{F}^{\dagger}_{\mathcal{A}}(k'_\perp - k_\perp) - (2\pi)^2 \delta(k'_\perp - k_\perp)) \,. \end{aligned} \tag{37}$$

A derivation is sketched in Appendix A. The main difference to the quark case lies in the eikonal factor, which is now taken in the adjoint representation,

$$F^{ab}_{\mathcal{A}}(x_\perp) \equiv \mathcal{A}(F(x_\perp))^{ab} \,. \tag{38}$$

The quark propagators $i/\not{p}$ and $-i/\not{l}$, where $l = q - p - k$, are treated in the high-energy approximation as explained in Sect. 3. The p_--integration implicit in A can be performed in such a way that p goes on shell in the first diagram of Fig. 3 and l goes on shell in the second diagram. The p_+- and k_+-integrations are performed using two of the three δ-functions from the amplitudes for the scattering off the external field. As a result of these manipulations the following expression is obtained,

$$S^a_\mu = eg \, 2\pi \delta(q_+ - p'_+ - k'_+ - l'_+) \int \frac{d^2p_\perp}{(2\pi)^2} \frac{d^2k_\perp}{(2\pi)^2} \frac{2q_+ \cdot \mathcal{M}_\mu \cdot C^a}{\left(Q^2 + \frac{p_\perp^2}{1-\alpha-\alpha'} + \frac{k_\perp^2}{\alpha'} + \frac{l_\perp^2}{\alpha}\right)} \,. \tag{39}$$

Here $\alpha = l_+/q_+$, $\alpha' = k_+/q_+$ and $\mathcal{M}_\mu$ describes the purely partonic part of the amplitude given by

$$\mathcal{M}_\mu = \bar{u}_{s'}(\bar{p}) \left[\gamma_\mu \frac{1}{\not{q} - \not{p}} \not{\varepsilon}_{(\lambda')}(k) - \not{\varepsilon}_{(\lambda')}(k) \frac{1}{\not{q} - \not{l}} \gamma_\mu \right] v_{r'}(\bar{l}) \,. \tag{40}$$

All the non-abelian eikonal factors are combined in C^a,

$$C^a = \int_{x_\perp, y_\perp, z_\perp} e^{i[x_\perp(p_\perp - p'_\perp) + y_\perp(k_\perp - k'_\perp) + z_\perp(l_\perp - l'_\perp)]} F(x_\perp, y_\perp, z_\perp)^a \,, \tag{41}$$

$$F(x_\perp, y_\perp, z_\perp)^a = \mathcal{A}(F^{\dagger}(y_\perp))^{ab} (F^{\dagger}(x_\perp) T^b F(z_\perp)) - T^a \,. \tag{42}$$

The last term in Eq. (42) subtracts the unphysical contribution where none of the partons is scattered by the external field (cf. Eq. (20)). One can think of $x_\perp, y_\perp$ and $z_\perp$ as the transverse positions at which quark, gluon and antiquark penetrate the proton field, picking up corresponding non-abelian eikonal factors.

4.2 Colour structure

In the phase space region with two of the three final state particles having high $p_\perp$, in the $\gamma^* p$ center-of-mass system, the form of the three-particle colour factor C^a simplifies

significantly. To see this, the three possible configurations, i.e. high-$p_\perp$ $q\bar{q}$-jets, high-$p_\perp$ qg-jets and high-$p_\perp$ $\bar{q}g$-jets, have to be distinguished.

Consider first the case of high-$p_\perp$ quark and antiquark, i.e. $p'^2_\perp$, $l'^2_\perp \gg \Lambda^2$. In analogy to the results of Sect. 3 a leading twist contribution to diffraction can only appear if the gluon is relatively soft, i.e. in the region of small $k'^2_\perp$ and α'. Therefore the relations $k'^2_\perp \sim \Lambda^2$ and $\alpha' \ll 1$ are used in the calculations below. This will also be justified by the final formulae, which show that these kinematical regions dominate the integrations.

The assumption of a smooth external field implies small transverse momentum transfer from the proton, i.e. $|p''_\perp| \sim \Lambda$, where $p''_\perp = p'_\perp - p_\perp$. The $p_\perp$-integration in Eq. (39) can be trivially replaced by a $p''_\perp$-integration, substituting at the same time

$$p_\perp = p'_\perp - p''_\perp \qquad \text{and} \qquad l_\perp = -p'_\perp + p''_\perp - k_\perp \,. \tag{43}$$

Neglecting $p''_\perp$ in $\mathcal{M}$ and in the energy denominator in Eq. (39), which is justified since $|p''^2_\perp| \ll |p'^2_\perp|, |l'^2_\perp|$, the only remaining $p''_\perp$-dependence is in the colour factor C^a. This simplifies the $p''_\perp$-integration to

$$\int \frac{d^2p''_\perp}{(2\pi)^2}\, C^a \,. \tag{44}$$

Defining $\Delta \equiv p' + k' + l' - p - k - l$ to be the total momentum transferred from the proton, C^a can be given in the from

$$C^a = \int_{x_\perp} e^{-ix_\perp\Delta_\perp} \int_{y_\perp,z_\perp} e^{i[y_\perp(k_\perp-k'_\perp)+z_\perp(l_\perp-l'_\perp)]} F(x_\perp, x_\perp+y_\perp, x_\perp+z_\perp)^a \,, \tag{45}$$

where $l_\perp$ is given by Eq. (43). The $p''_\perp$-integration gives a δ-function for the variable $z_\perp$, thus resulting in the final formula

$$\int \frac{d^2p''_\perp}{(2\pi)^2}\, C^a = \int_{x_\perp} e^{-ix_\perp\Delta_\perp} \int_{y_\perp} e^{iy_\perp(k_\perp-k'_\perp)} F(x_\perp, x_\perp+y_\perp, x_\perp)^a \,. \tag{46}$$

This result shows that in the kinematical situation with two high-$p_\perp$ quark jets and a relatively soft gluon the leading twist contribution is not affected by the transverse separation of the quarks. It is the transverse separation between quark-pair and gluon which tests large distances in the proton field and which can lead to non-perturbative effects.

The colour-singlet projection of the colour-tensor C reads

$$S(C) = \frac{1}{2}\,\mathrm{tr}[C^a T^a] \,. \tag{47}$$

Using the identity

$$\mathcal{A}(U)^{ab} = 2\ \mathrm{tr}[U^{-1}T^aUT^b] \quad , \quad U \in \mathrm{SU}(3)\,, \tag{48}$$

the contribution relevant for diffraction, i.e. the production of a colour-singlet $q\bar{q}g$-system, becomes

$$\int \frac{d^2p''_\perp}{(2\pi)^2}\ S(C) = \int_{x_\perp} e^{-ix_\perp\Delta_\perp}\ \frac{1}{4}\,\mathrm{tr}[\tilde{W}^{\mathcal{A}}_{x_\perp}(k_\perp - k'_\perp)]\,, \tag{49}$$

$$W^{\mathcal{A}}_{x_\perp}(y_\perp) = \mathcal{A}(F^\dagger(x_\perp + y_\perp)F(x_\perp)) - 1\,. \tag{50}$$

This is analogous to the quark-pair production of the previous section (cf. Eq. (20)). However, now the two lines probing the field at positions $x_\perp$ and $x_\perp + y_\perp$ correspond to matrices in the adjoint representation. An intuitive explanation of this result is that the two high-$p_\perp$ quarks are close together and are rotated in colour space like a vector in the octet representation. This situation is illustrated in Fig. 4.

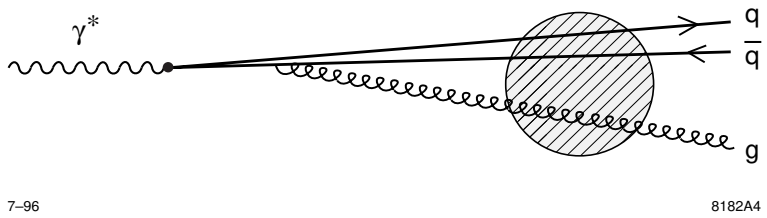

Fig.4 Space-time picture in the case of fast, high-$p_\perp$ quark and antiquark, passing the proton at small transverse separation with a relatively soft gluon further away.

To make this last statement more precise, recall that an upper bound for the Ioffe-time of the fluctuation with two high-$p_\perp$ quarks is given by $q_0/p_\perp^2$. This means that the distance between the point where the virtual photon splits into the $q\bar{q}$-pair and the proton can not be larger than $q_0/p_\perp^2$. As long as the pair shares the longitudinal momentum of the photon approximately equally, i.e. $\alpha(1-\alpha) = \mathcal{O}(1)$, the opening angle is $\sim p_\perp/q_0$. Therefore, the transverse distance between quark and antiquark is $\sim 1/p_\perp \ll 1/\Lambda$ when they hit the proton.

In the case where quark and gluon have high transverse momentum and the relatively soft, low-$p_\perp$ antiquark is responsible for the non-perturbative interaction, we have $|p'^2_\perp| \simeq |k'^2_\perp| \gg |l'^2_\perp| \sim \Lambda^2$ and $\alpha'' \equiv l_+/q_+ \ll 1$.

The calculation proceeds along the lines of the soft gluon case described previously. It is convenient to make the integration over the soft transverse momentum explicit by

substituting $d^2l_\perp$ for $d^2k_\perp$ in Eq. (39). The $p_\perp$-integration is replaced by a $p''_\perp$-integration and the $p''_\perp$-dependence entering $\mathcal{M}$ and the energy-denominator via the relations $p_\perp = p'_\perp - p''_\perp$ and $k_\perp = -p'_\perp + p''_\perp - l_\perp$ is neglected. The $p''_\perp$-integration gives a δ-function for the variable $y_\perp$, leading to the following result for the singlet projection of the colour tensor C,

$$\int \frac{d^2p''_\perp}{(2\pi)^2}\; S(C) = \int_{x_\perp} \; e^{-ix_\perp\Delta_\perp}\,\frac{2}{3}\,\mathrm{tr}[\tilde{W}_{x_\perp}(l_\perp - l'_\perp)]\,. \tag{51}$$

The function $W_{x_\perp}$ has been defined in Eq. (22). Now quark and gluon, having high transverse momentum, are close together and are colour rotated like a vector in the fundamental representation (see Fig. 5). Therefore, the colour structure of the amplitude is the same as for the quark-pair production of Sect. 3.

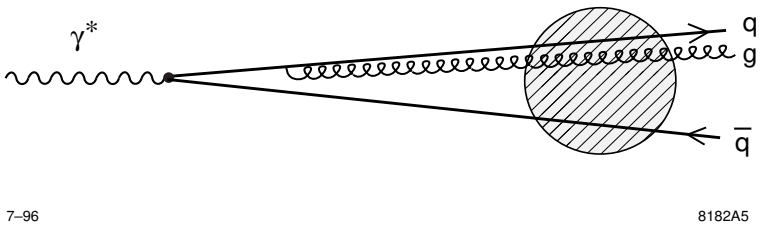

Fig.5 Space-time picture in the case of fast, high-$p_\perp$ quark and gluon, passing the proton at small transverse separation with a relatively soft antiquark further away.

The case of high-$p_\perp$ $\bar{q}g$-jets is completely analogous to the case of high-$p_\perp$ qg-jets and will not be discussed separately.

4.3 Longitudinal cross section

In the phase space region of $q\bar{q}$-jets with high transverse momentum described at the beginning of the previous subsection the phase space integration can be given in the form

$$\begin{aligned} d\Phi^{(3)} &= \frac{2}{(2\pi)^9}\,\frac{dp'_+}{2p'_+}d^2p'_\perp\frac{dk'_+}{2k'_+}d^2k'_\perp\frac{dl'_+}{2l'_+}d^2l'_\perp\delta(q_+ - p'_+ - k'_+ - l'_+) \\ &= \frac{1}{8(2\pi)^8}\,\frac{Q^2}{q_+x\alpha'}d\alpha d\alpha' d\xi d^2k'_\perp d^2\Delta_\perp\,. \end{aligned} \tag{52}$$

One obtains analogous expressions for the regions of high transverse momentum qg-and $\bar{q}g$-jets by replacing α' and $k'_\perp$ by the longitudinal momentum fraction and the transverse momentum of the soft parton.

Explicit formulae for the partonic part $\mathcal{M}$ of the amplitude defined in Sect. 4.1 are given in Appendix C. Treating the colour factors as described in the previous subsection explicit expressions for the different contributions to the longitudinal diffractive structure function are obtained. To stress the common features of these contributions from the different phase space regions generic kinematical variables are introduced. The longitudinal momentum fraction and the transverse momentum of one of the high-$p_\perp$ jets are denoted by γ and $r_\perp$ respectively. The longitudinal momentum fraction of the relatively soft parton is denoted by γ', its transverse momenta before and after the interaction with the external field are denoted by $s_\perp$ and $s'_\perp$. For example, in the case of quark and antiquark jets this notation means that $\gamma = \alpha$, $\gamma' = \alpha'$, $r_\perp = p_\perp$, $s_\perp = k_\perp$, and $s'_\perp = k'_\perp$.

The different contributions to F_L^D can be given in the form

$$F_L^{D,n}(x,Q^2,\xi) = \frac{16\alpha_S}{(2\pi)^5\xi}\,\beta^2(1-\beta)g_L^{(n)}(\beta)\int_0^1 d\gamma\,, \qquad n=1,2\,. \tag{53}$$

Here the contribution from the region of high-$p_\perp$ $q\bar{q}$-jets is labeled by $n=1$ and the sum of the contributions from the regions of high-$p_\perp$ qg- and $\bar{q}g$-jets is labeled by $n=2$. The trivial γ-integration has been kept explicitly to allow a more detailed description of the final states.

The β-spectrum can be different for the two contributions of Eq. (53). Its dependence on the details of the colour field of the proton is given by the two dimensionless functions

$$g_L^{(1)}(\beta) = \int_0^\infty \frac{(1+u)^2 u\,du}{32(\beta+u)^2}\int d^2s'_\perp (s'^2_\perp)^2 \int_{x_\perp}\left|\int \frac{d^2s_\perp}{(2\pi)^2}\cdot\frac{\mathrm{tr}[\tilde{W}^{\mathcal{A}}_{x_\perp}(s_\perp - s'_\perp)]\,t_L^{ij}}{s'^2_\perp(\beta+u)+s^2_\perp(1-\beta)}\right|^2 \tag{54}$$

$$g_L^{(2)}(\beta) = \int_0^\infty \frac{2(1+u)^2 du}{9(\beta+u)^2}\int d^2s'_\perp (s'^2_\perp) \int_{x_\perp}\left|\int \frac{d^2s_\perp}{(2\pi)^2}\cdot\frac{s_\perp\cdot\mathrm{tr}[\tilde{W}_{x_\perp}(s_\perp - s'_\perp)]}{s'^2_\perp(\beta+u)+s^2_\perp(1-\beta)}\right|^2, \tag{55}$$

where the tensor t_L^{ij} is given by

$$t_L^{ij} = \delta^{ij} + \frac{2s_\perp^i s_\perp^j}{s'^2_\perp}\cdot\frac{1-\beta}{\beta+u}\,, \qquad i,j=1,2\,. \tag{56}$$

Note, that in the modulus squared in Eq. (54) the appropriate contraction of the indices of the two tensors t_L^{ij} is assumed.

The integration variable u can be related to the old kinematic variables by

$$\gamma' = \frac{s'^2_\perp}{M^2}(1+u)\,. \tag{57}$$

The functions g_L^i have been given in terms of an integral in u to make it obvious that they do not depend on any kinematical variable other than β.

For the transverse momentum $r_\perp$ of the two hard jets the relation

$$r_\perp^2 = \gamma(1-\gamma)\left(M^2 - \frac{s_\perp'^2}{\gamma'}\right) = \gamma(1-\gamma)M^2\frac{u}{1+u} \tag{58}$$

can be derived. Using this relation and the γ- and u-distributions given by Eq. (53) and Eqs. (54),(55) the $r_\perp$-distribution of the jets in the final state can be easily recovered.

The above results show that within our model F_L^D has a leading twist contribution, suppressed by one power of α_S. For β not too close to 0 and 1 the integrals in γ and u are finite and dominated by the region where both γ and u are $\mathcal{O}(1)$. This justifies the assumption that $\gamma' \ll 1$ and $s_\perp'^2 \ll r_\perp^2$ made at the beginning of this section. Eq. (58) also shows that jets with transverse momentum of order M dominate F_L^D. This has to be contrasted with the case of transverse photon polarization, where the leading contribution comes from the production of a $q\bar{q}$-pair with small transverse momenta as discussed in Sect. 3.

The details of the β-spectrum and the $r_\perp$-distribution depend on the average over the proton field, which enters via non-abelian eikonal factors in the adjoint and fundamental representation (see Eqs. (54),(55)). This is a truly non-perturbative effect which, in our model, is responsible for leading twist diffraction. It is realized by one of the three produced partons, which is slower by a factor $\sim \Lambda^2/M^2$ and can develop a large transverse separation from the two other partons.

Let us finally consider the behaviour of the diffractive structure function at small β, i.e. at large invariant masses. The u-integration in $g_L^{(1)}(\beta)$ is divergent for $\beta = 0$. The behaviour of $g_L^{(1)}(\beta)$ at small β is determined by the integration over small values of u. This behaviour can be obtained assuming $\beta \ll 1$, $u \ll 1$ and $u + \beta \ll 1$ in Eq. (54). In this region the second contribution of the tensor t_L^{ij} in Eq. (56) dominates and the following expression for $g_L^{(1)}$ is obtained,

$$g_L^{(1)}(\beta \to 0) = \int_0^\infty \frac{u\,du}{8(\beta+u)^4} \int d^2s'_\perp \int_{x_\perp} \left| \int \frac{d^2s_\perp}{(2\pi)^2} \cdot \frac{\mathrm{tr}[\tilde{W}_{x_\perp}^{\mathcal{A}}(s_\perp - s'_\perp)]\; s_\perp^i s_\perp^j}{s_\perp^2} \right|^2 \tag{59}$$

$$= \frac{1}{48\beta^2} \int d^2s'_\perp \int_{x_\perp} \left| \int \frac{d^2s_\perp}{(2\pi)^2} \cdot \frac{\mathrm{tr}[\tilde{W}_{x_\perp}^{\mathcal{A}}(s_\perp - s'_\perp)]\; s_\perp^i s_\perp^j}{s_\perp^2} \right|^2 . \tag{60}$$

This means that $F_L^D(x,Q^2,\xi)$ approaches a constant value at fixed ξ and $\beta \to 0$. For the inclusive structure function, where one has to integrate over β, this implies a growth $\sim \ln(1/x)$. Since $g_L^{(2)}$ is less singular than $g_L^{(1)}$ at small β, the region of large diffractive masses is dominated by the configuration with high-$p_\perp$ $q\bar{q}$-jets and a relatively soft gluon.

4.4 Transverse cross section

The calculation of the diffractive contribution to the transverse structure function proceeds along the lines of the previous subsection, using the techniques described in Appendices B and C. However, due to the summation over photon polarizations the final formulae are somewhat more complicated. The result for the transverse diffractive cross section will be given using the generic kinematical variables introduced for the discussion of the longitudinal structure function above. Consider the contribution from the region of high-$p_\perp$ $q\bar{q}$-jets first,

$$F_T^{D,q\bar{q}} = \frac{4\alpha_S}{(2\pi)^5\xi}\,\beta(1-\beta)^2 g_T^{(1)}(\beta)\int_{\gamma_{min}}^{1-\gamma_{min}} d\gamma \frac{\gamma^2+(1-\gamma)^2}{\gamma(1-\gamma)}\,. \tag{61}$$

Note that the γ-integration has a logarithmic divergence in the region where quark or antiquark become soft, like the production of colour-octet $q\bar{q}$-pairs discussed in Sect. 3. Since our calculation is only reliable for $\gamma > \gamma' \sim \Lambda^2/Q^2$, the integration leads to a $\ln Q^2/\Lambda^2$ enhancement, which was absent in the leading order diffractive structure function given in Sect. 3.

The β-spectrum is determined by the dimensionless function

$$g_T^{(1)}(\beta) = \int_0^\infty \frac{(1+u)u^2\,du}{16(\beta+u)^2}\int d^2s'_\perp (s'^2_\perp)^2 \int_{x_\perp}\left|\int \frac{d^2s_\perp}{(2\pi)^2}\cdot\frac{\mathrm{tr}[\tilde{W}^{\mathcal{A}}_{x_\perp}(s_\perp - s'_\perp)]\,t_T^{ij}}{s'^2_\perp(\beta+u)+s_\perp^2(1-\beta)}\right|^2, \tag{62}$$

where

$$t_T^{ij} = e_\perp^i e_\perp^j - \frac{s_\perp^i s_\perp^j}{u s'^2_\perp} + \frac{(2e_\perp s_\perp)e_\perp^i s_\perp^j}{(\beta+u)s'^2_\perp}(1-\beta)\,, \tag{63}$$

and $e_\perp = r'_\perp/|r'_\perp|$ is an arbitrary unit vector, on which the integral does not depend. Contraction of the transverse tensor indices is assumed in Eq. (62).

It can be shown, following the discussion at the end of the last subsection, that $g_T^{(1)}(\beta) \sim 1/\beta$ at $\beta \to 0$, resulting in a constant behaviour of the diffractive structure function in this region. The same effect has previously been observed in [20], where the diffractive interaction with the proton is treated by means of 2-gluon exchange.

The sum of the contributions from the region of high-$p_\perp$ quark-gluon or antiquark-gluon jets is given by

$$F_T^{D,qg} = \frac{4\alpha_S}{(2\pi)^5\xi}\,\beta(1-\beta)^2 \int_{\gamma_{min}}^{1-\gamma_{min}} d\gamma \left[g_T^{(2)}(\beta) + \frac{1}{\gamma(1-\gamma)} g_T^{(3)}(\beta) + \frac{\gamma^3+(1-\gamma)^3}{\gamma(1-\gamma)} g_T^{(4)}(\beta) \right] , \quad (64)$$

where for $m = 2, 3, 4$ the functions $g_T^{(m)}(\beta)$ are defined by

$$g_T^{(m)}(\beta) = \int_0^\infty \frac{2(1+u)u\,du}{9(\beta+u)^2} \int d^2s'_\perp(s'^2_\perp) \int_{x_\perp} \left| \int \frac{d^2s_\perp}{(2\pi)^2} \cdot \frac{s_\perp \,\mathrm{tr}[\tilde{W}_{x_\perp}(s_\perp - s'_\perp)]\, t^{(m)}}{s'^2_\perp(\beta+u) + s^2_\perp(1-\beta)} \right|^2 , \quad (65)$$

$$t^{(2)} = 1 \quad , \quad t^{(3)} = \frac{s'^2_\perp(\beta+u)}{s'^2_\perp(1+u)\beta + s^2_\perp(1-\beta)} \quad , \quad t^{(4)} = t^{(2)} + t^{(3)} . \quad (66)$$

As in the longitudinal case, the contribution from the region with a high-$p_\perp$ gluon-jet is negligible at small β.

The results of the present section are the above explicit expressions for hard radiative corrections to the diffractive structure functions, calculated in the semiclassical approach of [8]. These radiative corrections yield high-$p_\perp$ jets, whereas the leading contribution is kinematically dominated by the aligned-jet configuration with small transverse momentum. This is similar to expectations based on the QCD-improved aligned-jet model [15].

Final states with high-$p_\perp$ jets in diffractive electroproduction have recently been also considered in [21, 22]. The main difference to our approach is the assumption of two-gluon exchange in these calculations. This leads to a different x-dependence of the jet cross sections.

5 Conclusions

It has been the purpose of this paper to investigate the applicability of the semiclassical approach to diffraction, to improve its technical implementation, and to extend it to the case of an additional final state gluon, radiated by the produced $q\bar{q}$-pair.

As has been shown in Sect. 2, the situation where the proton is scattered elastically can be described as quark-pair production in a given external colour field, averaging over all field configurations of the proton on the amplitude level. This averaging procedure has formally been defined using the Schrödinger wave functional of the proton.

The calculation of colour-singlet and colour-octet quark pair production in an external colour field had already been performed in [8]. In the present paper this calculation has been technically improved, thereby establishing its similarity to well-known light-cone techniques. This simpler technique made it possible to consider $\mathcal{O}(\alpha_S)$-corrections arising from an additional fast gluon in the final state. The cross sections for diffractive final states with a quark pair and one gluon have been given in the phase space region where two of the partons have large transverse momentum.

From these calculations an intuitive picture of leading twist diffraction emerges, which is very similar to Bjorken's aligned jet model. The leading contribution to both diffractive and non-diffractive deep inelastic events at small x is given by the process where the incoming virtual photon splits into a quark-pair long before the proton. When the quarks travel through the proton field they pick up non-abelian eikonal factors associated with their trajectory. These eikonal factors are sufficient to provide the small momentum transfer required to make the final state real.

If the relative transverse momentum of the quarks is large, the quarks have a small transverse separation when they travel through the proton field. Expanding in the transverse distance of the quarks it becomes obvious that the process is essentially perturbative and equivalent to one-gluon exchange. A constant contribution to F_L and a $\ln Q^2$ enhanced contribution to F_2 arise. No leading twist diffraction is possible.

If, however, the transverse momenta of the quarks are small, their trajectories pass the proton field at large transverse distance. The two eikonal factors test large transverse distances inside the proton making the process non-perturbative. The result is no longer equivalent to an exchange of a finite number of gluons. This gives a leading twist contribution to F_2 and F_2^D, the latter being interpreted as the fraction of events where the produced quark pair is in a colour-singlet state. Neither a $\ln Q^2$ enhancement of F_2^D nor a leading twist contribution to F_L^D are found.

The picture becomes more complicated when the radiation of an additional gluon is included. Now three eikonal factors test the proton field, corresponding to the trajectories of the two quarks and the gluon. The gluonic eikonal factor is in the adjoint representation. Leading twist diffractive processes appear when at least one of the three partons has small transverse momentum and carries a small fraction of the longitudinal momentum of the photon. The two other partons can have large transverse momentum. In this kinematical situation the two high-$p_\perp$ partons pass the field close together, acting effectively

as one particle. Therefore, only two Wilson lines test the proton field, analogously to the pure $q\bar{q}$-case. The corresponding colour rotation matrix is in the fundamental representation if the gluon combines with quark or antiquark, and in the adjoint representation if the two quarks combine to form a colour octet state.

The colour singlet projection of the $q\bar{q}g$-final state is interpreted as the diffractive contribution. As a result, leading twist, α_S-suppressed contributions to F_2^D and F_L^D are obtained. In the longitudinal case this is the leading diffractive process. It is dominated by configurations containing two jets with high transverse momentum, $|p_\perp| \sim M$, and is free from infrared divergences. No $\ln Q^2$ term appears. In the case of transverse polarization the diffractive cross section also contains a leading twist contribution from high-$p_\perp$ jets. However, now an infrared divergence appears in the region where the transverse momentum becomes small, leading to an $\alpha_S \ln Q^2$-term in the diffractive structure function.

Several qualitative phenomenological predictions can be derived from this picture of diffractive processes. Notice first, that the scaling violation associated with the $\ln Q^2$-terms appears in diffraction only in next-to-leading order. This means, that one would expect the ratio F_2^D/F_2 to decrease approximately like $\ln Q^2$. Also high-$p_\perp$ jets and diffraction of the longitudinally polarized photon appear only at order α_S. Therefore, in the $\gamma^* p$ center-of-mass system less high-$p_\perp$ jets should be visible in diffractive processes than in inclusive processes. It is, however, interesting to observe that F_L^D is, unlike F_2^D, dominated by high-$p_\perp$ jets.

The details of the β-spectrum and of the $p_\perp$-distribution of jets in diffractive processes depend on the average over the proton field configurations appearing in the semiclassical approach. They are given in terms of integrals over non-abelian eikonal factors testing the proton field. At small β the structure functions approach constants different from zero. In this region they are dominated by contributions from high-$p_\perp$ quark jets accompanied by a relatively soft gluon with small transverse momentum.

An important aspect of the semiclassical approach, which requires further study, is the energy dependence of the obtained cross sections. To leading order, the scattering in a classical background field yields a flat behaviour at small x, i.e., $F_2 \sim$ const. and $F_2^D \sim 1/\xi$. This corresponds to a classical bremsstrahl spectrum of gluons, $xg(x) =$const. The difference by one unit in the exponents of inclusive and diffractive structure functions is in agreement with our previous results [6, 8, 19], but certainly a stronger increase

is observed individually in both cases. Two potential sources for such an increase are loop corrections to the partonic part of our amplitude and radiation of additional gluons.

We would like to thank J. Bartels, M. Beneke, S.J. Brodsky and L. Frankfurt for valuable discussions and comments. A.H. has been supported by the Feodor Lynen Program of the Alexander von Humboldt Foundation.

Appendix A

In the following we shall give a brief derivation of the quark and gluon matrix elements used in Sect. 3 and Sect. 4.1.

Consider a fast moving particle with momentum l', where l'_+ is the large component. The wave function of an antiquark propagating through a colour field $G^a_\mu(x)$ satisfies the Dirac equation

$$(i\not{D} - m)\ \psi_v(x) = 0 \quad , \qquad D_\mu = \partial_\mu + iG_\mu \ . \tag{67}$$

An approximate solution for a fast antiquark in a 'soft' colour field, which approaches a plane wave solution with momentum l' of the free Dirac equation as $x^0 \to \infty$, is given by

$$\psi_v(x) = e^{il'x}\ V_0(x)\ v(l') \ , \tag{68}$$

where $\not{l}' v(l') = 0$ and

$$V_0(x) = P \exp\left(\frac{i}{2}\int_{x_+}^{\infty} dx'_+ G_-(x'_+, x_-, x_\perp)\right) \ . \tag{69}$$

Here colour indices of the spinor v and the matrix V_0 have been dropped. Corrections to this approximate solution are suppressed by powers of $1/l'_+$. Similarly, one obtains for a fast moving quark,

$$\bar\psi_u(x) = \bar u(l')\ U_0(x)\ e^{il'x} \ , \tag{70}$$

where $\bar u(l')\not{l}' = 0$ and

$$U_0(x) = P \exp\left(\frac{i}{2}\int_{\infty}^{x_+} dx'_+ G_-(x'_+, x_-, x_\perp)\right) \ = \ V_0^\dagger(x) \ . \tag{71}$$

The non-abelian phase factors satisfy the differential equations

$$l'\cdot D\ V_0 \ = \ U_0\ l'\cdot \overleftarrow{D} \ = \ 0 \ , \tag{72}$$

where $\overleftarrow{D}_\mu = \overleftarrow{\partial} - iG_\mu$.

The matrix element for the antiquark needed in Sect. 3 is now easily evaluated. Using Eq. (72) and $l' \simeq l$, $\bar v_r(l)\gamma^\mu v_{r'}(l') \simeq 2\ l^\mu \delta_{rr'}$, one obtains

$$\begin{aligned} T_{r,r'}(l,l') \ &= \ \int d^4y\ \bar v_r(l) e^{-ily} \not{G}(y)\psi_v(y) \\ &= \ \int d^4y\ e^{i(l'-l)y} \bar v_r(l) \not{G}(y)\ V_0(y)\ v_{r'}(l') \\ &\simeq \ 2il_+\delta_{rr'} \int d^4y\ e^{i(l'-l)y} \frac{\partial}{\partial y_+} V_0(y) \ . \end{aligned} \tag{73}$$

In Sections 3 and 4 we have considered diffractive masses $M = \mathcal{O}(Q)$. This implies for the momentum transfer, $l'_- - l_- \ll \Lambda$. Assuming, as discussed in Sect. 2, that the proton is localized at $y_3 \approx 0$, i.e. $y_+ = y_- + \mathcal{O}(1/\Lambda)$, we can then write

$$\begin{aligned} \int dy_+ \; e^{i(l'_- - l_-)y_+/2} \; \frac{\partial}{\partial y_+} V_0(y) \;\; &\simeq \;\; e^{i(l'_- - l_-)y_-/2} \; \int dy_+ \; \frac{\partial}{\partial y_+} \; V_0(y) \\ &= \;\; -\left(V_0(-\infty, y_-, y_\perp) - 1\right) \; . \end{aligned} \tag{74}$$

Inserting this in Eq. (73) yields the final result

$$T_{rr'}(l, l') = -2\pi i \; 2l_+ \delta_{rr'} \delta(l_+ - l'_+) \left(\tilde{F}(l_\perp - l'_\perp) - (2\pi)^2 \delta^2(l_\perp - l'_\perp) \right) \; , \tag{75}$$

where we have used $l_+ \delta(l_+ - l'_+) \simeq l_0 \delta(l_0 - l'_0)$, and

$$\begin{aligned} \tilde{F}(l_\perp - l'_\perp) \;\; &= \;\; \int_{y_\perp} \; e^{i(l_\perp - l'_\perp)y_\perp} F(y_\perp) \; , \\ F(y_\perp) \;\; &= \;\; P \exp\left(\frac{i}{2} \int_{-\infty}^{\infty} dy_+ G_-(y_+, y_-, y_\perp) \right) \; . \end{aligned} \tag{76}$$

A fast moving gluon can be treated similarly. The equation of motion for the gluon field reads,

$$\partial_\mu F_{\mu\nu} + i[A_\mu, F^{\mu\nu}] = 0 \; . \tag{77}$$

Expanding A_μ around the classical background field, $A_\mu \to G_\mu + A_\mu$, one obtains for a transverse gluon in the high energy approximation, where terms of order $1/l'_+$ are dropped, the wave equation

$$(\partial^2 - 2 \; l' \cdot G^{\mathcal{A}}) A_\mu = 0 \; . \tag{78}$$

Here $G^{\mathcal{A}}$ denotes the background field in the adjoint representation,

$$G^{\mathcal{A}}_\mu = G^a_\mu T^a \quad , \qquad T^a_{bc} = -i f_{abc} \; , \tag{79}$$

where f_{abc} are the SU(3) structure constants. A solution of Eq. (78) up to terms $\mathcal{O}(1/l'_+)$, which approaches a plane wave with momentum l' as $x^0 \to \infty$, is given by

$$A_\mu(x) = e^{il'x} \; V_0^{\mathcal{A}}(x) \; \varepsilon^*_\mu(l') \; , \tag{80}$$

where $l' \cdot \varepsilon^*(l') = 0$ and

$$V_0^{\mathcal{A}}(x) = \mathcal{A}(V_0(x)) = P \exp\left(\frac{i}{2} \int_{x_+}^{\infty} dx'_+ G^{\mathcal{A}}_-(x'_+, x_-, x_\perp) \right) \; . \tag{81}$$

Obviously, $V_0^{\mathcal{A}}$ satisfies the equation

$$l' \cdot D^{\mathcal{A}} \; V_0^{\mathcal{A}} = 0 \; . \tag{82}$$

The matrix element for the gluon, needed in Sect. 4.1, is now easily calculated. Inserting in the expression

$$T^g_{\lambda',\lambda} = \int d^4z \; A^{\mu}_{(\lambda')}(z) \; 2l \cdot G(z) \varepsilon_{(\lambda)\mu}(l) e^{-ilz} \tag{83}$$

the gluon wave function (80) yields the transition matrix element

$$T^g_{\lambda'\lambda}(l',l) = 2\pi i \, 2l_+ \delta_{\lambda'\lambda} \delta(l'_+ - l_+) \left(\tilde{F}^{\dagger}_{\mathcal{A}}(l'_\perp - l_\perp) - (2\pi)^2 \delta^2(l'_\perp - l_\perp) \right) \; . \tag{84}$$

Appendix B

The computation of longitudinal and transverse structure functions in Sect. 3 requires the evaluation of the product of an amplitude and its complex conjugate which depend on different transverse momenta, respectively. To evaluate these products, the following representation of spinors is useful (cf. [23]),

$$u_r(p) = \frac{\not{p} + m}{\sqrt{p_0 + m}} \; \varphi_r(m,0) \; , \; v_s(l) = \frac{-\not{l} + m}{\sqrt{l_0 + m}} \; \chi_s(m,0) \; . \tag{85}$$

This immediately yields,

$$u(\tilde{p})\bar{u}(p) = \frac{1}{\sqrt{(p_0+m)(\tilde{p}_0+m)}} (\not{\tilde{p}} + m) \frac{1+\gamma_0}{2} (\not{p} + m) \; , \tag{86}$$

$$v(l)\bar{v}(\tilde{l}) = -\frac{1}{\sqrt{(l_0+m)(\tilde{l}_0+m)}} (\not{l} - m) \frac{1-\gamma_0}{2} (\not{\tilde{l}} - m) \; , \tag{87}$$

where the sum over spins is understood. In the high energy expansion, and restricting ourselves to the massless case $m = 0$, one obtains

$$\begin{aligned} u(\tilde{p})\bar{u}(p) &= \frac{1}{2} p_+ \gamma_- + \frac{1}{2} p_- \gamma_0 \gamma_+ + \frac{1}{2} \tilde{p}_- \gamma_0 \gamma_- + p_\perp \gamma_\perp \; \gamma_- \frac{1-\gamma_0}{2} \\ &\quad - \tilde{p}_\perp \gamma_\perp \; \frac{1+\gamma_0}{2} \gamma_- + \frac{2}{p_+} \; \tilde{p}_\perp \gamma_\perp \; p_\perp \gamma_\perp \frac{1-\gamma_0}{2} \; + \; \mathcal{O}\left(\frac{1}{p_+^2} \right) \; , \end{aligned} \tag{88}$$

$$\begin{aligned} v(l)\bar{v}(\tilde{l}) &= \frac{1}{2} l_+ \gamma_- - \frac{1}{2} \tilde{l}_- \gamma_0 \gamma_+ - \frac{1}{2} l_- \gamma_0 \gamma_- - \tilde{l}_\perp \gamma_\perp \; \gamma_- \frac{1+\gamma_0}{2} \\ &\quad + l_\perp \gamma_\perp \; \frac{1-\gamma_0}{2} \gamma_- - \frac{2}{l_+} \; l_\perp \gamma_\perp \; \tilde{l}_\perp \gamma_\perp \frac{1+\gamma_0}{2} \; + \; \mathcal{O}\left(\frac{1}{l_+^2} \right) \; , \end{aligned} \tag{89}$$

where we have used $\tilde{p}_+ = p_+,\ \tilde{l}_+ = l_+$. It is now straightforward to evaluate the matrix elements needed for the longitudinal and the transverse structure functions. The results are, to leading order in the large momenta p_+ and l_+ $(i = 1, 2)$,

$$\mathrm{tr}\left[u(\tilde{p})\bar{u}(p)\gamma^0 v(l)\bar{v}(\tilde{l})\gamma^0\right] \;=\; 2\ p_+ l_+ \tag{90}$$

$$\mathrm{tr}\left[u(\tilde{p})\bar{u}(p)\gamma^i v(l)\bar{v}(\tilde{l})\gamma^i\right] \;=\; 4\ \frac{\alpha^2 + (1-\alpha)^2}{\alpha(1-\alpha)}\ p_\perp \tilde{p}_\perp\ . \tag{91}$$

The differential cross section for quark pair production reads

$$d\sigma_{\mu\nu} = \frac{2\pi}{q_+}\ T^*_\mu T_\nu\ d\Phi^{(2)}\ , \tag{92}$$

where T_μ is the amplitude given in Eq. (20), and $d\Phi^{(2)}$ is the phase space volume,

$$d\Phi^{(2)} = \frac{2}{(2\pi)^6}\ \frac{dp'_+}{2p'_+} d^2p'_\perp \frac{dl'_+}{2l'_+} d^2l'_\perp\ \delta(q_+ - p'_+ - l'_+)\ . \tag{93}$$

Changing variables,

$$p'_\perp = \Delta_\perp - l'_\perp\ , \quad l'_+ = \alpha q_+\ , \quad \xi = x\ \frac{Q^2 + M^2}{Q^2}\ , \tag{94}$$

using ${l'_\perp}^2 \simeq \alpha(1-\alpha)M^2$, and integrating over the orientation of $l'_\perp$, one obtains

$$d\Phi^{(2)} = \frac{1}{4(2\pi)^5}\frac{1}{q_+}\frac{Q^2}{x} d\alpha d\xi\ d^2\Delta_\perp\ . \tag{95}$$

Eqs. (20), (90) and (93) yield for the longitudinal structure function

$$dF_L \;=\; \frac{Q^2}{\pi e^2}\ d\sigma_L \;\simeq\; \frac{4Q^4}{\pi e^2 q_+^2}\ d\sigma_{00} \tag{96}$$

$$\;=\; \frac{4\ Q^6}{(2\pi)^7\beta}\ \frac{d\xi}{\xi}\ d\alpha\ (\alpha(1-\alpha))^3\ \int_{x_\perp}\left|\int d^2l_\perp \frac{\tilde{W}_{x_\perp}(l_\perp - l'_\perp)}{N^2 + l_\perp^2}\right|^2\ . \tag{97}$$

Here the integration over the transverse momentum $\Delta_\perp$ has been carried out. The integrand can be expanded around $l = l'$. Shifting the integration variable $l_\perp$ to $k_\perp = l_\perp - l'_\perp$, the Taylor expansion in powers of $k_\perp$ of the denominator yields

$$\frac{1}{N^2 + (k_\perp + l'_\perp)^2} = \frac{1}{N^2 + l'^2_\perp} - \frac{2k_\perp l'_\perp}{(N^2 + l'^2_\perp)^2}\ +\ \ldots\ . \tag{98}$$

From the definition of the colour matrix $W_{x_\perp}(y_\perp)$ in Eq. (22) it is clear that

$$\begin{aligned}\int d^2k_\perp\ \tilde{W}_{x_\perp}(k_\perp) \;&=\; W_{x_\perp}(0) \;=\; 0\ ,\\ \int d^2k_\perp\ k_\perp \tilde{W}_{x_\perp}(k_\perp) \;&=\; -i(2\pi)^2\ \partial_\perp W_{x_\perp}(0)\ .\end{aligned} \tag{99}$$

Using rotational invariance, i.e. $l'_i l'_j \to \frac{1}{2}\delta_{ij}\ l'^2_\perp$, and the relations

$$l'^2_\perp \simeq \alpha(1-\alpha)\frac{1-\beta}{\beta}Q^2\ , \quad N^2 + l'^2_\perp \simeq \alpha(1-\alpha)\frac{Q^2}{\beta}\ , \tag{100}$$

one obtains the final result (26).

The transverse structure function can be evaluated in a similar way. Summing over the transverse polarizations and using the matrix element (91), one obtains

$$\begin{aligned} dF_T &= \frac{Q^2}{\pi e^2}\ \frac{1}{2}\sum_{\lambda=1,2}\varepsilon^{*(\lambda)}_\mu \varepsilon^{(\lambda)}_\nu\ d\sigma^{\mu\nu} = \frac{Q^2}{\pi e^2}\ \frac{1}{2}\ d\sigma^{ii} \\ &= \frac{8\ Q^4}{(2\pi)^7\beta}\ \frac{d\xi}{\xi}\ d\alpha\ \alpha(1-\alpha)(\alpha^2+(1-\alpha)^2)\int_{x_\perp}\left|\int d^2 l_\perp \frac{l_\perp \tilde{W}_{x_\perp}(l_\perp - l'_\perp)}{N^2 + l^2_\perp}\right|^2 . \end{aligned} \tag{101}$$

Performing again a Taylor expansion in $k_\perp = l_\perp - l'_\perp$ and using rotational invariance, one obtains the expression (27), which is similar to (26). The expansion is valid for $\alpha > \Lambda^2/Q^2$. Integration over α in the range Λ^2/Q^2 to $1/2$ yields the factor $\ln Q^2/\Lambda^2 - 1$.

In contrast to F_L there is an additional contribution to F_T, which is most easily discussed in the case of diffraction, where

$$W_{x_\perp}(y_\perp) \to \frac{1}{\sqrt{3}}\ \mathrm{tr}[W_{x_\perp}(y_\perp)]\ . \tag{102}$$

Because of $\partial_\perp \mathrm{tr}[W_{x_\perp}(0)] = 0$, only the region of small α yields a leading twist contribution to F_2^D. Defining a new integration variable ρ by

$$\alpha = \frac{\beta}{Q^2}\ \rho^2\ , \tag{103}$$

and using $1 - \alpha \simeq 1$,

$$N^2 \simeq \beta\ \rho^2\ , \quad |l'_\perp| \simeq \rho\ \sqrt{1-\beta}\ , \tag{104}$$

one obtains the expression (33),(34) for F_2^D. Since in the integral for F_2^D large values of α do not contribute at leading twist, the integration over ρ can be extended to ∞. The complete expression for the inclusive structure function F_T, including the function $f(\beta)$ of Eq. (29), can be obtained analogously, but without taking the trace over $W_{x_\perp}(y_\perp)$.

Appendix C

Here we give some technical details of the calculation leading to the diffractive contributions of Sections 4.3 and 4.4. The main problem is the calculation of the partonic part $\mathcal{M}$

of the amplitude given by Eq. (39). In the following, the necessary manipulations will be described for the longitudinal cross section in the case of high-$p_\perp$ quark-antiquark jets. A complete derivation of $F_L^{D,1}$, Eq. (53), is obtained. For the other diffractive contributions only the results for the corresponding partonic parts $\mathcal{M}$ will be given.

The longitudinal cross section can be calculated using the relation $\sigma_L = (Q^2/q_0^2)\sigma_{00}$. Therefore it is sufficient to calculate $\mathcal{M}$, given by Eq. (40), for the unphysical photon polarization $\epsilon(q) = (1, \vec{0})$,

$$\mathcal{M}_0 = \bar{u}_{s'}(\bar{p}) \left[\gamma_0 \frac{\not{q} - \not{\bar{p}}}{(q-\bar{p})^2} \not{\epsilon} - \not{\epsilon} \frac{\not{q} - \not{\bar{l}}}{(q-\bar{l})^2} \gamma_0 \right] v_{r'}(\bar{l}) \,. \tag{105}$$

Here $\epsilon_{\lambda'}(k) = \epsilon$ has been used for brevity. The high-energy approximation for the quark propagator introduced in Sect. 3 (see in particular Eqs. (15),(16)) corresponds to the replacements

$$\not{q} - \not{\bar{p}} \;\simeq\; \not{\bar{l}} + \not{k} = \sum_\rho v_\rho(\bar{l}) \bar{v}_\rho(\bar{l}) + \not{k} \tag{106}$$

$$\not{q} - \not{\bar{l}} \;\simeq\; \not{\bar{p}} + \not{k} = \sum_\rho u_\rho(\bar{p}) \bar{u}_\rho(\bar{p}) + \not{k} \,. \tag{107}$$

Note, that k is an on-shell vector. Furthermore, it can be shown that the terms proportional to $\not{k}$ are suppressed in Eq. (105) in the limit $k_\perp^2 \ll p_\perp^2 \simeq l_\perp^2$, $\alpha' \ll 1$, which corresponds to the case of high-$p_\perp$ $q\bar{q}$-jets. Making use of the relations

$$\bar{u}_{s'}(\bar{p}) \not{\epsilon} u_\rho(\bar{p}) = (2\bar{p}\epsilon)\delta_{s'\rho} \quad , \quad \bar{v}_\rho(\bar{l}) \not{\epsilon} v_{r'}(\bar{l}) = (2\bar{l}\epsilon)\delta_{\rho r'} \tag{108}$$

the following expression for $\mathcal{M}_0$ can be derived,

$$\mathcal{M}_{0,q\bar{q}} = 2\bar{u}_{s'}(\bar{p}) \gamma_0 v_{r'}(\bar{l}) \left(\frac{\bar{l}\epsilon}{(q-\bar{p})^2} - \frac{\bar{p}\epsilon}{(q-\bar{l})^2} \right) . \tag{109}$$

Here the index $q\bar{q}$ specifies the considered kinematical region of high-$p_\perp$ quark and antiquark.

With $\epsilon_- = 2\epsilon_\perp k_\perp / k_+$, which follows from $\epsilon k = 0$, the relations

$$\bar{l}\epsilon = \frac{\alpha}{\alpha'} \epsilon_\perp k_\perp - \epsilon_\perp l_\perp \quad , \quad \bar{p}\epsilon = \frac{1-\alpha}{\alpha'} \epsilon_\perp k_\perp - \epsilon_\perp p_\perp \tag{110}$$

are obtained. The denominators in Eq. (109) can be given in the form

$$(q-\bar{p})^2 \simeq -\alpha N^2 \quad , \quad (q-\bar{l})^2 \simeq -(1-\alpha)N^2 \left(1 + \frac{2k_\perp p_\perp}{\alpha(1-\alpha)N^2} + \mathcal{O}(k_\perp^2) \right) , \tag{111}$$

where

$$N^2 = Q^2 + \frac{p_\perp^2}{\alpha(1-\alpha)}\,. \tag{112}$$

Although the term $\sim k_\perp$ in Eq. (111) is small compared to the leading term, it can not be neglected. In combination with the term $\sim k_\perp/\alpha'$ of Eq. (110) it will give a finite contribution of order $k_\perp^2/\alpha'$.

Inserting (110) and (111) into Eq. (109) and keeping only the leading contributions the following formula for $\mathcal{M}_{0,q\bar{q}}$ is obtained,

$$\mathcal{M}_{0,q\bar{q}} = \frac{2\bar{u}_{s'}(\bar{p})\gamma_0 v_{r'}(\bar{l})}{\alpha(1-\alpha)N^2}\left(\epsilon_\perp p_\perp + \frac{(2\epsilon_\perp k_\perp)(p_\perp k_\perp)}{\alpha' N^2}\right)\,. \tag{113}$$

Notice, that $\mathcal{M}_{0,q\bar{q}}$ depends on the intermediate gluon momentum k and the integration over this variable has to be performed independently for the amplitude and its complex conjugate. Therefore, we do actually not need the square of $\mathcal{M}_{0,q\bar{q}}$ but the product $\mathcal{M}^*_{0,q\bar{q}}(k)\mathcal{M}_{0,q\bar{q}}(\tilde{k})$. Here k and $\tilde{k}$ are two independent integration variables. Summing over transverse gluon polarizations and quark and antiquark helicities the following result is derived,

$$\sum_{\lambda' s' r'} \mathcal{M}^*_{0,q\bar{q}}(k)\mathcal{M}_{0,q\bar{q}}(\tilde{k}) = \frac{8q_+^2}{\alpha(1-\alpha)N^4}\left(p_\perp + k_\perp\frac{(2p_\perp k_\perp)}{\alpha' N^2}\right)\left(p_\perp + \tilde{k}_\perp\frac{(2p_\perp \tilde{k}_\perp)}{\alpha' N^2}\right)\,. \tag{114}$$

Using this expression and the colour factor of Eq. (49) together with the amplitude (39) and the phase space formula (52) the cross section σ_L can be calculated. Note, that in Eqs. (54), (55) the phase space integration over $\alpha' = \gamma'$ has been substituted by an integration over u, defined in Eq. (57).

For the other possible kinematical configurations in both the longitudinal and the transverse case similar techniques can be used to perform the calculation of $\mathcal{M}$. In the following we simply state the results for the polarization sums over $\mathcal{M}^*(k)\mathcal{M}(\tilde{k})$. The kinematical variables are the same as in Sect. 4.

For the longitudinal cross section in the case of high-$p_\perp$ quark and gluon jets the following polarization sum is required,

$$\sum_{\lambda' s' r'} \mathcal{M}^*_{0,qg}(l)\mathcal{M}_{0,qg}(\tilde{l}) = \frac{4(1-\alpha)q_+^2}{N^4}\frac{l_\perp \tilde{l}_\perp}{\alpha''}\,. \tag{115}$$

To derive $F_L^{D,2}$, Eq. (53), the contribution from high-$p_\perp$ antiquark-gluon jets has to be added, which is proportional to α and renders the cross section independent of the momentum fraction.

The diffractive contribution to the transverse structure function from the region of high-$p_\perp$ quark and antiquark jets can be calculated from

$$\frac{1}{2}\sum_{i=1,2}\sum_{\lambda' s' r'}\mathcal{M}^*_{i,q\bar{q}}(k)\mathcal{M}_{i,q\bar{q}}(\tilde{k}) = \frac{8(\alpha^2+(1-\alpha)^2)}{\alpha(1-\alpha)N^4}\times \tag{116}$$

$$\times\left(\frac{p^i_\perp p^j_\perp}{\alpha(1-\alpha)} - \frac{k^i_\perp k^j_\perp}{\alpha'} + \frac{(2p_\perp k_\perp)p^i_\perp k^j_\perp}{\alpha(1-\alpha)N^2\alpha'}\right)\left(\frac{p^i_\perp p^j_\perp}{\alpha(1-\alpha)} - \frac{\tilde{k}^i_\perp \tilde{k}^j_\perp}{\alpha'} + \frac{(2p_\perp \tilde{k}_\perp)p^i_\perp \tilde{k}^j_\perp}{\alpha(1-\alpha)N^2\alpha'}\right).$$

In the case of high-$p_\perp$ quark and gluon the corresponding contribution reads

$$\frac{1}{2}\sum_{i=1,2}\sum_{\lambda' s' r'}\mathcal{M}^*_{i,qg}(l)\mathcal{M}_{i,qg}(\tilde{l}) = \frac{4p^2_\perp(l_\perp \tilde{l}_\perp)}{\alpha(1-\alpha)N^4\alpha''}\times \tag{117}$$

$$\times\left[\alpha+\frac{1}{\alpha}\left(\frac{N^2}{Q^2+l^2_\perp/\alpha''}\right)\left(\frac{N^2}{Q^2+\tilde{l}^2_\perp/\alpha''}\right)+\frac{(1-\alpha)^2}{\alpha}\left(1+\frac{N^2}{Q^2+l^2_\perp/\alpha''}\right)\left(1+\frac{N^2}{Q^2+\tilde{l}^2_\perp/\alpha''}\right)\right].$$

Together with the formulae of Sections 4.1 and 4.2 the remaining results of Sections 4.3 and 4.4 follow in a straightforward manner.

References

[1] ZEUS collaboration, M. Derrick et al., Phys. Lett. B315 (1993) 481; Z. Phys. C68 (1995) 569

[2] H1 collaboration, T. Ahmed et al., Nucl. Phys. B429 (1994) 477; Phys. Lett. B348 (1995) 681

[3] J. D. Bjorken and J. Kogut, Phys. Rev. D8 (1973) 1341

[4] G. Ingelman and P. Schlein, Phys. Lett. B152 (1985) 256;
A. Donnachie and P. V. Landshoff, Phys. Lett. B191 (1987) 309; Nucl. Phys. B303 (1988) 634

[5] A. H. Mueller, Nucl. Phys. B335 (1990) 115;
M. G. Ryskin, Sov. J. Nucl. Phys. 52 (1990) 529;
N. N. Nikolaev and B. G. Zakharov, Z. Phys. C53 (1992) 331

[6] W. Buchmüller and A. Hebecker, Phys. Lett. B355 (1995) 573

[7] A. Edin, G. Ingelman and J. Rathsman, Phys. Lett. B366 (1996) 371

[8] W. Buchmüller and A. Hebecker, DESY 95-208 (1995), to appear in Nucl. Phys. B

[9] Yu. L. Dokshitzer, V. A. Khoze, A. H. Mueller and S. I. Troyan, *Basics of Perturbative QCD* (Editions Frontières, Gif-sur-Yvette, 1991)

[10] J. D. Bjorken, J. Kogut and D. E. Soper, Phys. Rev. D3 (1971) 1382

[11] O. Nachtmann, Ann. Phys. 209 (1991) 436

[12] H.G. Dosch, E. Ferreira and A. Krämer, Phys. Rev. D50 (1994) 1992;
I.A. Korchemskaya and G.P. Korchemsky, Nucl. Phys. B437 (1995) 127;
L.N. Lipatov, Nucl. Phys. B452 (1995) 369

[13] I. Balitsky, Nucl. Phys. B463 (1996) 99

[14] M. Lüscher, Nucl. Phys. B254 (1985) 52

[15] L. Frankfurt and M. Strikman, Phys. Rep. 160 (1988) 235

[16] H. Abramowicz, L. Frankfurt and M. Strikman, Proc. of the SLAC Summer Institute 1994, p. 539

[17] J. D. Bjorken, *Rapidity Gaps in Deep Inelastic Scattering*, Conf. on Fund. Int. of Elementary Particles, Moscow, 1995, SLAC-PUB-7096 (1996)

[18] J. Ellis and G. G. Ross, *Can one probe the structure function of the pomeron?*, CERN-TH/96-101 (1996)

[19] W. Buchmüller, Phys. Lett. B353 (1995) 335

[20] J. Bartels and M. Wüsthoff, J. Phys. G22 (1996) 929

[21] M. Diehl, Z. Phys. C66 (1995) 181

[22] J. Bartels, H. Lotter and M. Wüsthoff, Phys. Lett. B379 (1996) 239

[23] C. Itzykson and J.-B. Zuber, *Quantum Field Theory*, McGraw-Hill, New York, 1980